AIP Journal of Applied Physics

On the origin of photogenerated terahertz radiation from current-biased superconducting YBa 2 Cu 3 O 7 thin films

Po-Iem Lin, Chih-Wei Luo, Hsin-Shan Liu, Shyh-Feng Chen, Kaung-Hsiung Wu, Jenh-Yih Juang, Tseng-Ming Uen, Yih-Shung Gou, and Jiunn-Yuan Lin

Citation: Journal of Applied Physics **95**, 8046 (2004); doi: 10.1063/1.1738537
View online: http://dx.doi.org/10.1063/1.1738537
View Table of Contents: http://scitation.aip.org/content/aip/journal/jap/95/12?ver=pdfcov
Published by the AIP Publishing

JOURNAL OF APPLIED PHYSICS VOLUME 95, NUMBER 12 15 JUNE 2004

On the origin of photogenerated terahertz radiation from current-biased superconducting $YBa_2Cu_3O_{7-\delta}$ thin films

Po-Iem Lin,[a] Chih-Wei Luo, Hsin-Shan Liu, Shyh-Feng Chen, Kaung-Hsiung Wu, Jenh-Yih Juang, Tseng-Ming Uen, and Yih-Shung Gou
Department of Electrophysics, National Chiao Tung University, Hsinchu, Taiwan

Jiunn-Yuan Lin
Institute of Physics, National Chiao Tung University, Hsinchu, Taiwan

(Received 19 December 2003; accepted 18 March 2004)

The origin of photogenerated terahertz radiation pulse emitted from current-biased superconducting $YBa_2Cu_3O_{7-\delta}$ thin films excited by femtosecond optical laser pulses is delineated. By investigating the performance of the transient terahertz radiation generated under different operating parameters, pulse reshaping in the measured terahertz electric field caused by the kinetic inductance of the superconducting charge carriers is identified. After recovering the original wave forms of the emitted terahertz pulses, the transient supercurrent density directly correlated to the optically excited quasiparticle dynamics is obtained. A fast decreasing component of about 1.0 ps and a slower recovery process with a value of 2.5 ps are unambiguously delineated in the optically induced supercurrent modulation. The radiation mechanism of the transient terahertz pulse related to nonequilibrium superconductivity is discussed.
[DOI: 10.1063/1.1738537]

INTRODUCTION

The ultrafast photoresponse of high-T_c superconductors (HTSCs) has attracted much attention due to its unique capacity in uncovering the nonequilibrium dynamics of the optically excited quasiparticles. The photoinduced transient reflectivity change measured by the optical pump-probe method has identified two distinct characteristic relaxation times in the superconducting state, linked to the information of the energy gap.[1] Using a subpicosecond electro-optic sampling system, the typical nonequilibrium kinetic-inductance photoresponse of voltage transient[2] was ascribed to the nonequilibrium quasiparticle generation and recombination in the presence of an applied dc bias current.[3]

Recently, the modulation of kinetic inductance by ultrafast laser pulses has been utilized as a sampling technique for measuring ultrafast electric wave forms.[4] On the other hand, the reshaping of terahertz (THz) pulses upon transmission through superconducting thin films caused by the kinetic inductance of the superconducting charge carriers was detected by using coherent THz time-domain spectroscopy.[5,6] In general, the kinetic inductance of charge carriers is neglected since the intrinsic impedance is usually dominated by the resistance. In a superconducting state, however, the kinetic inductance becomes more significant and must be considered as an important parameter. This pulse reshaping effect is, unfortunately, mostly ignored (unintentionally) in interpreting the observed picosecond electromagnetic pulses emitted from optically excited superconducting bridges, which have revived interest in using HTSC films as potential THz radiation sources.[7–9] As a result, depending on the radiation and detection schemes employed, there have been discrepancies in trying to directly associate the resultant pulse shape with the characteristic times of the optically induced quasiparticle generation and recombination. Furthermore, although THz radiation based on the supercurrent modulation has been proposed,[8] the radiation mechanism of photogenerated THz radiation is still obscure because it is largely inconsistent with the characteristics of optically excited quasiparticle dynamics obtained by femtosecond time-resolved spectroscopy.

Coherent THz radiation emitted from biased photoconductive switches has been investigated and explained as follows.[10,11] The externally biased constant voltage drives the photogenerated carriers to form a transient photocurrent across the field region. A radiated THz electric field is obtained by the time derivative of the net current. It acts as the source term in Maxwell's equation, given as

$$\mathbf{E}_{\mathrm{THz}} \propto \frac{\partial \mathbf{J}}{\partial t}. \tag{1}$$

It is natural to suggest that the amplitude of transient THz electric field in superconducting films can be similarly interpreted as the time derivative of the supercurrent density. The dynamics of the quasiparticles optically induced by the ultrafast laser pulses then determines the performance of the transient THz radiation generated under different operating parameters. Since the THz electric field is measured at the backside of substrate, the pulse may be reshaped by the kinetic inductance of the superconducting charge carriers before reaching the detector. In this article we report the observation of THz generation from superconducting $YBa_2Cu_3O_{7-\delta}$ (YBCO) thin films by using a free-space electro-optic sampling (FSEOS) technique. By taking into account of the effect of kinetic inductance on the pulse re-

[a]Electronic mail: glinpi.ep87g@nctu.edu.tw

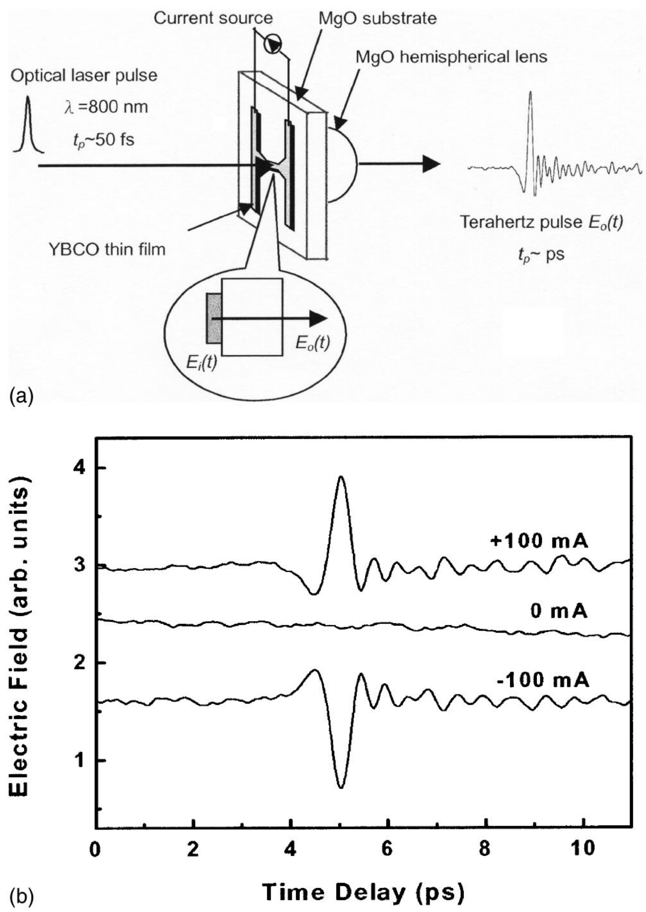

FIG. 1. (a) Schematic diagram of the free-space THz generation in the experimental setup in which t_p is pulse duration of either laser or THz pulse. The enlarged portion denotes the matter of the original THz pulses $E_i(t)$ and the reshaping of THz pulses $E_o(t)$ that transmission through the superconducting YBCO film and substrate in the time domain. (b) Measured transient THz radiation from superconducting YBCO bow-tie antenna at 50 K. The polarity of the THz wave forms measured with bias currents of +100 mA and −100 mA. No signal is observed when zero bias current is applied.

shaping, our results demonstrate the direct connection between the quasiparticle dynamics and the detected THz radiation. Indeed, by transforming the pulse shape back to the original circumstance, the time integral of the original THz pulse reveals a fast decreasing component of about 1.0 ps and a slower recovery process, with a value of 2.5 ps for the optically induced supercurrent modulation, consistent with that obtained from the optical reflectivity measurements. These results not only remove the discrepancies just mentioned, but also indicate that the THz generation is a direct manifestation of quasiparticle dynamics in response of the optical excitations.

EXPERIMENTAL DETAILS

Schematics of the experimental setup are shown in Fig. 1(a). YBCO thin films were deposited on 0.5-mm-thick MgO(100) substrates by pulsed-laser deposition. The films were *c*-axis oriented, and had a typical thickness of 110 nm for the THz generation experiments. The YBCO thin films were patterned into a bow-tie antenna structure using standard photolithography and wet chemical etching. The center bridge is 200 μm long and 100 μm wide with the bow-tie angle of 60°. The critical temperature T_c was 88 K after patterning into the antenna structure and the critical current densities (J_c) were 1.7×10^6 A/cm^2 at 77 K and 1.0×10^7 A/cm^2 at 50 K. In addition, for optical reflectivity measurements, 300-nm-thick YBCO film was deposited on $SrTiO_3(100)$ substrate. The details of the optical setup of transient reflectance ($\Delta R/R$) measurements were similar to those reported previously.[12]

The generation and detection of THz radiation was realized by using FSEOS technique. A cw argon-laser-pumped, compact, mode-locked Ti:sapphire laser (Femtosource C20) provides 20-fs optical pulses at 800 nm (1.55 eV) with a 75 MHz repetition rate. The pump beam focused into a spot size about 50 μm in diameter was modulated by a mechanical chopper which operated at 1.3 kHz and incident normal to the center bridge of YBCO bow-tie antenna. The electric field of the THz pulse was sampled by scanning the delay between the pump and probe beam. The superconducting YBCO bow-tie antenna, triggered by femtosecond optical laser pulses, radiates the THz signals. The THz radiation emitted through the backside of the MgO substrate was collimated by an MgO hemispherical lens with a diameter of 5 mm attached to the backside of the substrate. The THz radiation was then passed through a 3-mm-thick vacuum window made of Teflon™ and focused by a pair of off-axis paraboloidal mirrors onto the 1.0-mm-thick ZnTe(110) sensor crystal. For low-temperature measurements, the samples were cooled using a Janis flow-through cold-finger cryostat. In the detection segment, the orientation dependence of THz beam detection in ZnTe crystal was accomplished by using an undoped semi-insulating GaAs (SI-GaAs) photoconductive switch. The shape of THz pulses remains, but the peak amplitude of the signal and the polarity vary with the probe beam polarization and the THz beam polarization with respect to the (001) axis of the (110)-oriented ZnTe crystal. The results were then used to determine the optimal operating parameters for our THz detection setup. Further details of the experimental setup can be found in our previous publication.[9]

RESULTS AND DISCUSSION

The typical photogenerated THz radiation (THz electric field pulse $E_{\rm THz}$) as a function of the scanning delay time obtained from a current-biased superconducting YBCO bow-tie antenna measured at 50 K is shown in Fig. 1(b). The optical excitation power was 190 mW and the biased currents were +100 mA, 0 mA, and −100 mA, respectively. A sharp pulse about 450 fs wide is observed. The figure also shows that the polarity of the THz electric field is reversed by reversing the bias current direction, and that no signal is observed when no bias current is applied, revealing the essentiality of the optically induced transient supercurrent density. This consequence can be understood from Eq. (1), in which the change of photocurrent with time can be treated as the supercurrent transient in superconductors.

We note that in order to describe the generation of the THz radiation, two major points have to be clarified. The first

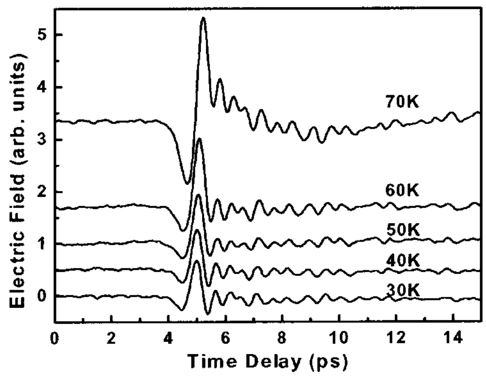

FIG. 2. Temperature dependence of emitted THz wave forms. The excitation power is 190 mW. The dramatic change in pulse shape is shown in the figure.

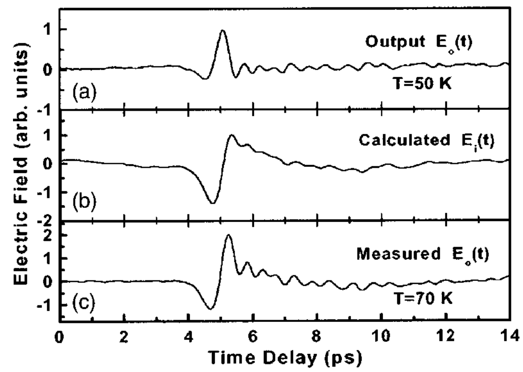

FIG. 3. (a) Measured (output) THz pulse $E_o(t)$ at 50 K, (b) original THz pulse $E_i(t)$ obtained by Eq. (3) using the data in (a), and (c) measured THz pulse at 70 K.

one is the carrier dynamics giving rise to the generation of the THz electric field pulse, and the other one is the output coupling of the radiation from the superconducting thin films. The dynamics of the emitted THz transient related to the nonequilibrium superconductivity is investigated by measuring the dependence of the radiation on optical excitation power, bias current, and ambient temperature. The peak strength of the transient THz radiation was found to increase linearly with optical excitation power as well as the bias current, indicating the superradiant character of the emission.[9] Next, it would be interesting to see whether the wave form changes with ambient temperature. Figure 2 shows a series of emitted THz pulses obtained at several temperatures. The phase and the shape of the transient change significantly at different ambient temperatures. It is evident that the shape of the transient terahertz pulses is almost the same in each case, except for the 70 K results, in which the shape after the main pulse followed a slower component with a characteristic time of about 2.5 ps. It is noted that the phase of the pulse also shifts with increasing the temperature. With regard to the peak amplitude of THz signals, the radiation amplitude rapidly increases with increasing temperature. This phenomenon has been attributed to the reduced superconductor energy gap and associated temperature-dependent transmission and absorption coefficients.[7]

As far as classical electromagnetic dynamics is concerned, a far-field radiated THz electric field is proportional to the time derivative of the net current. From the results just presented it is natural to suggest that the THz electric field E_{THz} from YBCO films is generated by the temporal modulation of the supercurrent density $\partial J_s/\partial t$. Within the framework of the two-fluid model, the bias current density J_s can be described as

$$J_s = 2en_s\nu_s, \tag{2}$$

where e is the charge of the carrier; J_s is expected to change when an optical transient is illuminated at the bridge region. The time derivative of J_s thus gives a transient wave form of the induced radiation. On the other hand, the time integral of the observed E-field amplitude correspondently gives the current transient in the time domain. An unphysical time scale was obtained, however, if one interprets the transient wave forms shown in Fig. 2 as direct manifestation of $\partial J_s/\partial t$. The response time obtained this way appears to be too fast for supercurrent transient associated with quasiparticle dynamics. Similar difficulties have been encountered when trying to assign the subpicosecond recovering time to quasiparticle recombination response time,[3,8] which is about an order of magnitude shorter than normally conceived values.[1,12]

In general, the frequency-dependent conductivity $\sigma_s(\omega)$ of the superconducting carriers is purely imaginary, indicating that the superconducting films may act as an ideal inductor. This property is referred to as kinetic inductance, since the effect is a consequence of the superconducting carrier's kinetics.[2,13,14] The phase sensitivity of the THz pulse spectrometer allows us to observe directly the kinetic inductance of the carriers. The results are illustrated in Fig. 3, which shows the time-domain spectroscopy taken on the YBCO film at 50 K. The output (measured) electric field of the THz pulse is determined by the response of the film and the dielectric properties of the substrate. MgO substrate turns out to be an excellent material with sufficiently low loss to allow for the extended propagation of subpicosecond electromagnetic pulses. The influence of the substrate on pulse shape can be neglected. Notice that there is a dramatic change of the pulse shape in Figs. 3(a) and 3(c) for results measured at 50 K and 70 K, respectively. In order to yield the original THz pulse [$E_i(t)$ denoted in the enlarged graph of Fig. 1(a)], which emitted from the superconducting microbridge, propagated through the superconducting film itself, passed through the substrate and lens, and then transmitted to the free space, the output THz electric field $E_o(t)$ is transformed via a transfer function. The transfer function $T(\omega)$, relating the original pulse $E_i(\omega)$ and output pulse $E_o(\omega)$, is expressed as[5]

$$T(\omega) = \frac{E_o(\omega)}{E_i(\omega)} \propto (-i\omega), \tag{3}$$

where the pulse $E_o(t)$ is Fourier transformed to get $E_o(\omega)$, divided by $(-i\omega)$, and inversely Fourier transformed to yield $E_i(t)$.

The calculated pulse $E_i(t)$ (the original one) is shown in Fig. 3(b). *This original pulse has the shape of the initial THz* *electric field that is not affected by the kinetic inductance of superconducting film itself*. It is interesting to note that the recovered pulse [Fig. 3(b)] has a wave form similar to the 70 K result [Fig. 3(c)]. It is indicative that for the 70 K result, due to having fewer participating superconducting charge carriers, the effect of kinetic inductance is insignificant. (With the excitation power illuminated in the region of the superconducting bridge, a rise of about 10 K is estimated to drive the actual sample temperature to near T_c.) It appears that the pulse reshaping is a direct result of the superconductor's kinetic inductance. Moreover, the phase of the transient also changes significantly in the time domain and is consistent with that reported earlier.[15]

As can be seen in Fig. 2, the phase shift of the propagated transient is roughly 240 fs below T_c. Taking the absorption coefficient $\alpha = 1.1\times 10^{-5}$ cm^{-1} for YBCO thin films, an optical penetration depth of $\delta = 1/\alpha \sim 90$ nm above T_c is estimated.[16] The value of δ will rapidly reduce upon decreasing temperature below T_c due to the variations in the heat capacity as well as the temperature transient irradiated by the laser pulse. We note that, in the more established coherent THz time-domain spectroscopy technique, which uses SI-GaAs photoconductive switch as the THz radiation source, similar pulse reshaping of transient THz was observed (not shown here) from a 30-nm-thick YBCO film deposited on $NdGaO_3$ substrate. In that case, the pulse reshaping was modeled as a transmission line shunted by an inductor having an impedance $Z = -i\omega L$ to act as a high-pass filter.[5] In principle, the inductance L as a function of temperature must be taken into account in the transfer function $T(\omega)$ in Eq. (3). In particular, since YBCO is known to have *d*-wave pairing, the nodal regions can lead to strong temperature dependence of the kinetic inductance even well below T_c.[17] However, in our case, although L may affect the absolute pulse amplitude, it does not change the genuine characteristics of the radiation. This explains the essentially similar behaviors observed for temperatures below 60 K. For the 70 K result, the influence of temperature-dependent inductance and the enhanced optical penetration depth in the superconductor sets in, leading to a very different behavior shown in Fig. 2.

Following the previous discussion, the temperature dependence of the original THz pulses from YBCO films are obtained and shown in Fig. 4. The fact that all the recovered pulses exhibit almost the same behavior not only lends strong support to our previous conjectures, but also is indicative of one essential underlying mechanism. Since Eq. (1) implies that the optically induced transient of the supercurrent density in the time domain can be subsequently obtained by integrating the recovered emitted electric field pulses as long as the supercurrent transient is the only prominent mechanism giving rise to the observed radiation.

In Fig. 5, we briefly recap the main observations described so far. With no bias current, no THz radiation is observed [Fig. 5(a)], indicating again the important role played by the supercurrent density. Figure 5(b) shows the pulse directly detected which presumably has been reshaped by the kinetic inductance. By using the transfer function expressed in the form of Eq. (3), the recovered pulse is depicted in Fig. 5(c). Finally, the irradiated *E*-field pulse is integrated over the sampling time to obtain the supercurrent density transient ΔJ_s. As is evident from Fig. 5(d), ΔJ_s apparently exhibits two characteristic time scales: a descending time of about 1 ps and a rising time of about 2.5 ps. If we attribute ΔJ_s to be associated mainly with quasiparticle dynamics, the two characteristic times should correspond to multiple excitation of hot-carrier thermalization-induced supercarrier reduction and to quasiparticle recombination to recover supercarriers, respectively. The latter usually is related to the superconducting energy gap and has been employed ubiquitously in pump-probe measurements to infer energy gap evolutions.

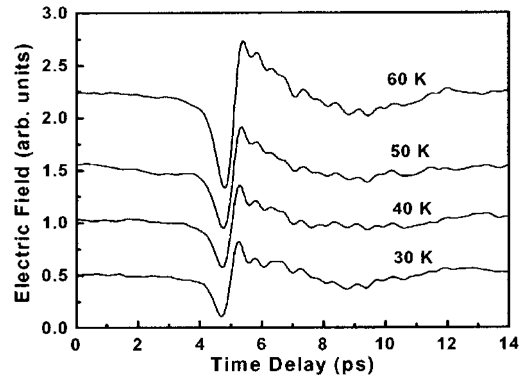

FIG. 4. Temperature dependence of the recovered THz pulses calculated from the data in Fig. 2 and the transfer function.

Usually, the optical reflectivity measured by the optical pump-probe method has a femtosecond time response, while the gap opening is manifested by a rapid increase in the amplitude of the photogenerated transient reflectance in the superconducting state. The ultrafast rise of the reflectivity after excitation of the YBCO is attributed to Cooper pairs breaking, and the subsequence decrease of the reflectivity results from quasiparticle relaxation. Below T_c, the logarithmic plots of $\Delta R/R$ reveal a break in slope near $t = 2.5$ ps. Two relaxation processes[1,12] (fast component τ_1 and slow component τ_2) in our measured data can be clearly observed in YBCO films, as shown in the Fig. 6(b). In this case, the two-component fit to the data yields two relaxation times

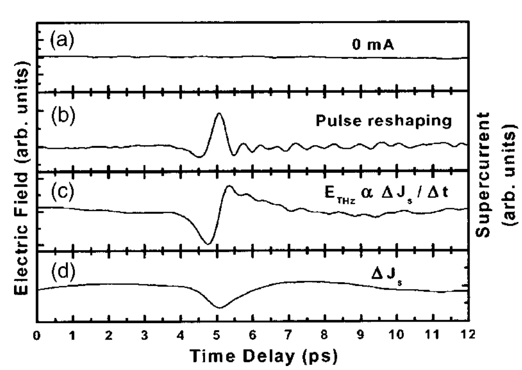

FIG. 5. A recap of THz generation related to nonequilibrium superconductivity: (a) no THz signal with zero bias current, (b) the detected "raw" terahertz radiation, (c) the recovered terahertz radiation after removing the kinetic inductance effect, and (d) the "actual" supercurrent transient obtained by integrating the recovered radiation pulses.

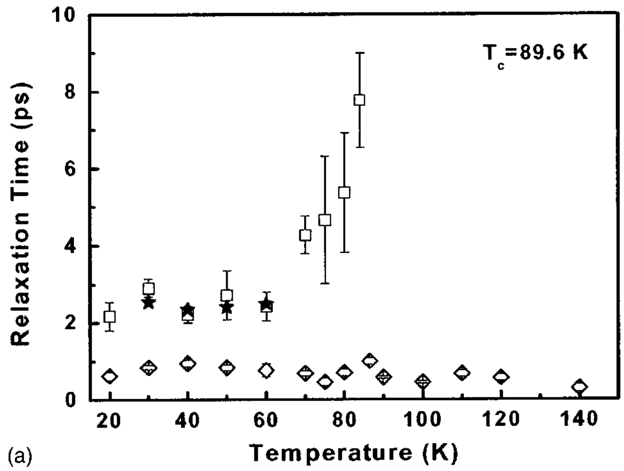

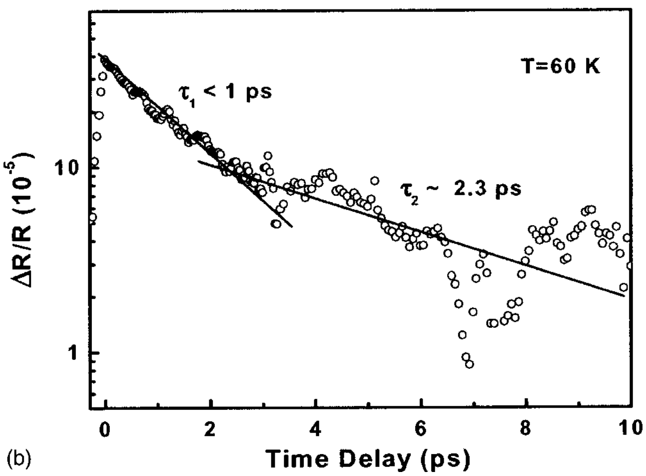

FIG. 6. (a) The two temperature-dependent relaxation times obtained from optical reflectivity transient measurements in YBCO films. The fast component τ_1 (◇) in subpicosecond range appears to be insensitive to temperature, while the slow component τ_2 (□) diverging near T_c is frequently attributed to gap opening. The characteristic time of quasiparticle recombination calculated from THz generation results (30–60 K) denoted by (⋆) is also included for comparison. (b) The typical reflectivity transient $\Delta R/R$ data used to obtain τ_1 and τ_2. The solid line is drawn to indicate the trend.

with $\tau_1 \sim 0.7$ ps and $\tau_2 \sim 2.3$ ps at 60 K. Figure 6(a) shows the typical temperature dependence of relaxation times τ_1 and τ_2 for YBCO films obtained by pump-probe measurements. For comparison, we also include the quasiparticle recombination characteristic time obtained from the recovered ΔJ_s curves at various temperature [⋆ in Fig. 6(a)]. The consistency between the two independent measurements is remarkable. It is noted that the fast relaxation process of about 1.0 ps in pump-probe $\Delta R/R$ is also very close to the present ΔJ_s descending time scale.

Finally, we turn our attention to the 70 K result [Fig. 3(c)]. The pulse appears to be only slightly modified by kinetic inductance due to drastic suppression of superconducting carriers when $T \rightarrow T_c$. Thus, it is difficult to identify an appropriate transfer process to remove the reshaping effect. Nonetheless, by comparing with the reshaped and recovered pulses at lower temperatures [Figs. 3(a) and 3(b)], the oscillation tail following the main pulse is suggestive of a reshaping effect. Although there have been suggestions that the oscillation tails in various THz radiations may have arisen from the absorption of atmospheric water vapor,[18] the fact that it can be significantly suppressed by removing the kinetic inductance effect indicates the antenna circuit itself might be important as well. Analyses along this direction are in progress and will be reported separately.[19]

CONCLUSIONS

In conclusion, we report a free-space electro-optic sampling of the terahertz pulse generation from current-biased superconducting YBCO thin films with excitations of femtosecond optical laser pulses. The effect of the kinetic inductance originated from the superconducting charge carriers is identified to be solely responsible for the pulse reshaping of the original terahertz pulse. The distorted pulses inevitably result in unphysical time scales, which, in turn, have prevented a direct interpretation relating the supercurrent density transient-induced radiation to quasiparticle dynamics. By including a proper transfer function to remove the effect of kinetic inductance and to recover the original shape of the radiation pulses, we have been able to relate the quasiparticle dynamics associated with nonequilibrium superconductivity to the photogenerated THz radiation in a consistent and physically plausible fashion.

ACKNOWLEDGMENTS

This work was supported by the National Science Council of Taiwan, R.O.C. under grant NSC 92-2112-M-009-031.

1 J. Demsar, B. Podobnik, V. V. Kabanov, Th. Wolf, and D. Mihailovic, Phys. Rev. Lett. **82**, 4918 (1999).
2 N. Bluzer, Phys. Rev. B **44**, 10222 (1991); J. Appl. Phys. **71**, 1336 (1992).
3 C. Williams, R. Adam, Q. Xie, R. Sobolewski, and O. Harnack, Semicond. Sci. Technol. **12**, 843 (1999).
4 C. J. Stevens, G. Bianchi, and J. F. Ryan, Appl. Phys. Lett. **82**, 4014 (2003).
5 S. D. Brorson, R. Buhleier, J. O. White, I. E. Trofimov, H.-U. Habermeier, and J. Kuhl, Phys. Rev. B **49**, 6185 (1994).
6 R. A. Kaindl, M. A. Carnahan, J. Orenstein, D. S. Chemla, H. M. Christen, H.-Y. Zhai, M. Paranthaman, and D. H. Lowndes, Phys. Rev. Lett. **88**, 027003 (2002).
7 C. Jaekel, H. G. Roskos, and H. Kurz, Phys. Rev. B **54**, 6889 (1996).
8 M. Hangyo, S. Tomozawa, Y. Murakami, M. Tonouchi, M. Tani, Z. Wang, K. Sakai, and S. Nakashima, Appl. Phys. Lett. **69**, 2122 (1996).
9 P. I. Lin, K. H. Wu, J. Y. Juang, J.-Y. Lin, T. M. Uen, and Y. S. Gou, IEEE Trans. Appl. Supercond. **13**, 20 (2003).
10 J.-H. Son, T. B. Norris, and J. F. Whitaker, J. Opt. Soc. Am. B **11**, 2519 (1994).
11 D. Grischkowsky, S. Keiding, M. Van Exter, and C. Fattinger, J. Opt. Soc. Am. B **7**, 2006 (1990).
12 C. W. Luo, M. H. Chen, C. C. Chiu, S. P. Chen, K. H. Wu, J.-Y. Lin, J. Y. Juang, T. M. Uen, and Y. S. Gou, J. Low Temp. Phys. **131**, 767 (2003).
13 M. C. Nuss, P. M. Mankiewich, M. L. O'Malley, E. H. Westerwick, and P. B. Littlewood, Phys. Rev. Lett. **66**, 3305 (1991).
14 S. D. Brorson, R. Buhleier, I. E. Trofimov, J. O. White, Ch. Ludwig, F. F. Balakirev, H.-U. Habermeier, and J. Kuhl, J. Opt. Soc. Am. B **13**, 1979 (1996).
15 M. C. Nuss, K. W. Goossen, P. M. Mankiewich, and M. L. O'Malley, Appl. Phys. Lett. **58**, 2561 (1991).
16 F. A. Hegmann and J. S. Preston, Phys. Rev. B **48**, 16023 (1993).
17 A. Sergeev and M. Reizer, Int. J. Mod. Phys. **10**, 635 (1996).
18 R. A. Cheville and D. Grischkowsky, Opt. Lett. **20**, 1646 (1995).
19 P. I. Lin, K. H. Wu, J. Y. Juang, J.-Y. Lin, T. M. Uen, and Y. S. Gou (unpublished).